HHS Public Access

Author manuscript

Alcohol Clin Exp Res. Author manuscript; available in PMC 2015 April 01.

Published in final edited form as:

Alcohol Clin Exp Res. 2013 August ; 37(8): 1333–1342. doi:10.1111/acer.12098.

Ethanol inhibition of a T-type Ca^{2+}channel through activity of protein kinase C

Hong Qu Shan, PhD[a]

[a]Department of Neurobiology and Anatomy, Wake Forest University School of Medicine, Winston-Salem, NC 27157, USA

James A. Hammarback, PhD[a]

[a]Department of Neurobiology and Anatomy, Wake Forest University School of Medicine, Winston-Salem, NC 27157, USA

Dwayne W. Godwin, PhD[a,b]

[a]Department of Neurobiology and Anatomy, Wake Forest University School of Medicine, Winston-Salem, NC 27157, USA

[b]Department of Neuroscience Program, Wake Forest University School of Medicine, Winston-Salem, NC 27157, USA

Abstract

Background—T-type calcium channels are widely distributed in the central and peripheral nervous system, where they mediate calcium entry and regulate the intrinsic excitability of neurons. T-channels are dysregulated in response to alcohol administration and withdrawal. We therefore investigated acute ethanol effects and the underlying mechanism of action in Human Embryonic Kidney (HEK) 293 cell lines, as well as effects on native currents recorded from dorsal root ganglion (DRG) neurons cultured from Long-Evans Rats.

MATERIALS and Methods—Whole cell voltage-clamp recordings were performed at 32-34°C in both HEK cell lines and DRG neurons. The recordings were taken after a 10 min application of ethanol or protein kinase C (PKC) activator (phorbol 12-myristate 13-acetate, PMA).

Results—We recorded T-currents from three channel isoforms ($Ca_V3.1$, $Ca_V3.2$ and $Ca_V3.3$) before and during administration of ethanol. We found that only one isoform, $Ca_V3.2$, was significantly affected by ethanol. Ethanol reduced current density as well as producing a hyperpolarizing shift in steady state inactivation of both $Ca_V3.2$ currents from HEK 293 cell lines and in native T currents from DRG neurons that are known to be enriched in $Ca^V3.2$. A protein kinase C peptide inhibitor (MPI) blocked the major ethanol effects, in both the cell lines and the DRG neurons. However, PMA effects were more complex. Lower concentration PMA (100 nM) replicated the major effects of ethanol, while higher concentration PMA (1 μM) significantly increased current density, suggesting that the ethanol effect may operate at lower PKC activation levels.

Corresponding author: Dr. Dwayne W. Godwin, Department of Neurobiology and Anatomy, Wake Forest University School of Medicine, 1 Medical Center Boulevard, Winston Salem NC, 27157, USA, dgodwin@wakehealth.edu, Phone: 1- (336)716-9437, Fax: 1-(336)716-4534.

Conclusions—Ethanol primarily affects the $Ca_V3.2$ isoform of T-type Ca^{2+}channels acting through PKC, highlighting a novel target and mechanism for ethanol effects on excitable membranes.

Keywords

ethanol; protein kinase C; phorbol 12-myristate 13-acetate; $Ca_V3.2$ T channel; dorsal root ganglion

---

T-type calcium channels (T-channels) are involved in numerous physiological processes throughout the body. In the nervous system, T-channels serve as both a portal for Ca^{2+} entry as well as a regulator of neuronal excitability (Perez-Reyes, 2003), contributing to burst firing and sleep rhythms (Huguenard and McCormick, 1992). Inappropriate calcium entry through T-channels has been linked to several pathophysiological disorders such as epilepsy, chronic pain and hypertension (Chen et al., 2010; Graef et al., 2009; Nelson et al., 2006; Ohishi et al., 2007).

Studies of acute ethanol administration have shown disruption of native T-currents in thalamic slice preparations (Mu et al., 2003), as well as long term disruption of T-channel expression and function upon withdrawal following chronic, intermittent ethanol exposures (Graef et al., 2011). Our prior studies were performed in preparations in which native currents were affected. However, the isolation and study of the various T-type currents are important, because native currents may comprise currents generated through three structurally heterogeneous and functionally distinctive T-channels [($Ca_V3.1$ (a1G), $Ca_V3.2$ (a1H) and $Ca_V3.3$ (a1I)] (Chemin et al., 2001; Cribbs et al., 1998; Lee et al., 1999; Monteil et al., 2000; Perez-Reyes et al., 1998).

T - channels can be isolated in expression systems, as well as in dorsal root ganglion (DRG) neurons, where they mediate sensory and pain responses (Coste et al., 2007). Small and medium DRG neurons contain both $Ca_V3.1$ and $Ca_V3.2$ channels, although $Ca_V3.2$ predominates (Talley et al., 1999), thus DRG neurons are an ideal neuronal preparation to probe for $Ca_V3.2$ specific effects. General anesthetics, including ethanol, block recombinant and native T-type Ca^{2+} currents (T-currents) in peripheral and central neurons (Joksovic et al., 2005a,b; Todorovic and Lingle, 1998; Todorovic et al., 2000). An inducible knockdown of $Ca_V3.2$ reduced T-currents in DRG neurons, resulting in antinociceptive effects, suggesting that $Ca_V3.2$ is important in the processing of pain and may constitute a target of anesthetics (Bourinet et al., 2005).

In the present study, we investigated the effects of ethanol on each of the three T-channel isoforms expressed in human embryonic kidney (HEK) 293 cell lines (Lee et al., 1999), as well as the underlying cellular mechanisms. Our study shows that $Ca_V3.2$ is a target for ethanol effects in neuronal systems, and illustrates the essential role of protein kinase C (PKC) in modifying T channel activity.

MATERIALS AND METHODS

Recombinant Human Embryonic Kidney Cells

HEK 293 cell lines stably expressing the human a1G ($Ca_V3.1$), a1H ($Ca_V3.2$), a1I ($Ca_V3.3$) were generous gifts from Dr. Edward Perez-Reyes (University of Virginia Health System). Cell lines were maintained in Dulbecco's modified Eagle medium (1X, DMEM), supplemented with 10% Fetal Bovine Serum (Invitrogen, Carlsbad, CA), 100 U/ml penicillin and 100 ug/ml streptomycin (Invitrogen), and 0.5 mg/ml Geneticin 418 using a 37°C, 5% CO_2 incubator. Cells were typically used 2–4 days after plating. Barium was used as a charge carrier to substitute for Ca^{2+} to record T-type currents. Standard extracellular solution for recording consisted of (in mM):124 NaCl, 5 KCl, 2.0 $MgCl_2$, 10 Glucose, 23 $NaHCO_3$, 1.5 NaH_2PO_4, 2 $BaCl_2$, with pH adjusted to 7.4 with HCl. The internal pipette solution for patch recordings consisted of (in mM):110 Trizma trisphosphate diabasic, 28 Trizma base, 11 EGTA, 2 $MgCl_2$, 0.1 $CaCl_2$, 4 Na_2-ATP, with pH adjusted to 7.2~7.3 using phosphoric acid. All recordings were performed with whole cell patch-clamp techniques at 32-34°C. Myristoylated protein kinase C peptide inhibitor (MPI: 50 μM, Promega Corporation, Madison, WI) was added to the internal solution. Phorbol 12 - myristate 13-acetate (PMA: 100 nM and 1μM, Sigma Chemical) was made from a concentrated stock and added to the artificial cerebrospinal fluid (ACSF).

Dissociated DRG Cultures

All animal experiments were approved by the Institutional Animal Care and Use Committee (IACUC) of Wake Forest University and in agreement with National Institutes of Health and United States Department of Agriculture guidelines, including practices to eliminate suffering and reduce animal numbers to the extent possible. Thirty male Long-Evans rats (30 days old, Harlan Laboratories, Indianapolis, IN, USA) were anesthetized with isoflurane. DRG cell culture was performed as previously described (Coste et al., 2007). Standard whole-cell patch clamp recordings were typically made after one to three days in culture. Standard extracellular solution for recording consisted of (in mM):124 NaCl, 5 KCl, 2 $MgCl_2$, 10 Glucose, 23 $NaHCO_3$, 1.5 NaH_2PO_4, 2 $BaCl_2$, 0.0005 TTX, 0.008 Nimodipine, 0.02 $CdCl_2$ with pH adjusted to 7.4 with HCl. The internal pipette solution for whole cell patch recordings consisted of (in mM): 130 CsCl, 10 HEPES, 10 EGTA, 8 NaCl, 1 $CaCl_2$, 1 $MgCl_2$, 4 Na_2ATP, 10 QX314 bromide with pH adjusted to 7.3 with CsOH. Recordings were made with standard whole cell patch clamp techniques.

Drugs and chemicals

Tetrodotoxin (TTX, 0.0005 mM, Alomone Labs, Jerusalem, Israel), nimodipine (0.008mM, Sigma Chemical), cadmium chloride ($CdCl_2$, 0.02mM, Sigma Chemical), QX314 (10 mM, Tocris Biosciences, Ellisville, MO), Myristoylated protein kinase C peptide inhibitor (MPI: 0.05mM, sequence: Myr-Arg-Phe-Ala-Arg-Lys-Gly-Ala-Leu-Arg-Gln-Lys-Asn-Val, Promega Corporation, Madison, WI) was added to the internal solution. 10^{-4} and 10^{-3} mM phorbol 12 -myristate 13- acetate (PMA, Sigma Chemical) were made from a concentrated stock and added to the ACSF.

Electrophysiology

Whole cell patch clamp recordings were performed at 32-34°C. Cellular activity was acquired with an Axopatch 200B amplifier (Molecular Devices, Sunnyvale, CA) in voltage-clamp mode, Brownlee 410 preamplifier (Palo Alto, CA) and CV 203 BU headstage (Molecular Devices, Sunnyvale, CA), and digitized with a Digidata 1440A (Molecular Devices). Patch pipettes (6–10 MΩ) were pulled using a Sutter Instrument Co. P-87 (Novato, CA). The bath temperature was kept at 32-34°C via a temperature controller (Warner, Hamden, CT). Current inactivation was achieved by 1s voltage step commands from −135 mV to −60 mV followed by a 500 ms test pulse at −50 mV.

Analysis

Average peak inactivation and activation currents were normalized to the peak of the maximally available current (I/I_{max}). This normalized current was plotted as a function of prepulse potential, and fitted with a Boltzmann equation: $I = I_{max}/ (1 + \exp [(V - V_{50})/k])$ by least-squares fits to derive, the half-maximal voltage (V_{50}) (Coulter et al., 1989; Crunelli et al., 1989). Each recorded current provides a unique Boltzmann fit, and the mean derived V_{50} and K values for all cells in a given cohort were used for comparison between groups. The decay constants of the first trace of elicited T-type Ca^{2+} currents for all voltage-clamp recorded cells were fitted in Clampfit 10.2 (Molecular Devices) with a standard exponential decay function.

$$I(t) = \sum_{i}^{n} A_i * exp(-t/T_i) + c$$

Net charge was calculated by integrating the total area of the first trace of elicited current for each cell. Two-way, One-way ANOVA and paired *t*-test were used to assess the significance of population effects using Prism 4 (GraphPad Software Inc. La Jolla, CA) with an alpha level of 0.05.

RESULTS

We used whole-cell patch-clamp recordings to determine the effects of ethanol on $Ca_V3.1$, $Ca_V3.2$ and $Ca_V3.3$ channels from HEK cell lines, respectively. To assess the effects of ethanol on kinetic properties of three isoforms of T channels, inactivation curves resulting from the voltage command protocols were fitted to the Boltzmann equation.

Ethanol Affects $Ca_V3.2$, but not $Ca_V3.1$ and $Ca_V3.3$ Channel Isoforms

Measurements were obtained after ten minutes of bath application to allow drug effects to achieve steady state. We found that ethanol (100 mM) significantly shifted the inactivation curve to a more hyperpolarized membrane potential in $Ca_V3.2$ channels (Fig. 1A,B), but not in $Ca_V3.1$ or $Ca_V3.3$ channels (Fig. 1C, D). The V_{50} (membrane potential at which half the current is available) derived from the inactivation curve shifted to a more negative membrane potential but it did not change in $Ca_V3.1$ or $Ca_V3.3$ currents (n=11, $p<0.01$, paired *t*-test, Fig. 1E). Ethanol reduced current amplitude, but because the current amplitude

can be affected by the size of the cell, we also measured current density by normalizing the whole cell current to cell capacitance and found that current density was reduced significantly, but not in $Ca_V3.1$ or $Ca_V3.3$ channels (n =10, $p<0.05$, paired *t*-test, Fig. 1F). The reduction of current density was consistent with the shift in the inactivation curve, resulting in the inhibition of the current. The I-V curve measurements also showed 32% reduction of the peak current after application of ethanol (Fig. 1H). The V_{50} derived from the activation curve showed no significant differences after administration of 100 mM ethanol (Fig. 1I).

Dose Dependency of Ethanol Effects on $Ca_V3.2$

After determining a clear and selective effect of ethanol on $Ca_V3.2$ channels at high intoxicating levels, we studied the dose-dependency of ethanol effects on this isoform at five concentrations (10–200 mM). We used one-way ANOVA to confirm a homogeneous baseline for current density between the groups ($F_{4,62}=2.308$, one-way ANOVA, $p>0.05$). We compared the current density before and after applying each concentration of ethanol and found that 50, 100 and 200 mM ethanol significantly decreased current density ($F_{1,74}=28.76$, $p<0.0001$, 2-way ANOVA; $p<0.01$, $p<0.0001$, and $p<0.05$, respectively, Bonferroni post hoc test, Fig. 2Bi). In order to normalize variation in the baseline we expressed the current obtained during ethanol relative to the control current measured in the same cell. We found that 100 and 200 mM ethanol significantly reduced current density ($F_{5,74}=8.494$, $p<0.0001$, 1-way ANOVA; $p<0.01$ and $p<0.05$, respectively, Dunnett's post hoc test, Fig. 2Bii).

PKC Mediation of Ethanol Effects on T-type Current

A myristoylated PKC peptide inhibitor (MPI: 50 μM) was delivered through the internal pipette solution (There was no significant differences between the baselines of the two groups with or without PKC inhibitor in the internal solution). We then concurrently applied 100 mM ethanol to the cells. We found a significant main effect of ethanol on V_{50} ($F_{1,20}=16.99$, $p=0.0005$, 2-way ANOVA) and a significant interaction between ethanol and MPI treatment ($F_{1,20}=6.972$, $p=0.0157$, 2-way ANOVA). Ethanol significantly shifted V_{50} to a more negative membrane potential ($p<0.001$, Bonferroni post hoc test) but it did not affect V_{50} when MPI was added in the internal solution ($p>0.05$, Bonferroni post hoc test, Fig. 3C). This illustrated that the PKC inhibitor blocked the hyperpolarizing shift in the inactivation curve (Fig. 3A, B). Ethanol significantly reduced rise time ($F_{2,24}=7.739$, $p=0.0025$, 2-way ANOVA; $p<0.01$, Bonferroni post hoc test, Fig. 3D), decay constant ($F_{2.26}=3.899$, $p=0.0330$, 2-way ANOVA; $p<0.01$, Bonferroni post hoc test, Fig. 3E) and current density ($F_{1,18}=9.564$, $p=0.0063$, 2-way ANOVA; $p<0.05$, Bonferroni post hoc test Fig.3F). We also found a significant interaction in decay constant between ethanol and MPI treatments ($F_{2.26}=7.729$, $p=0.0023$, 2-way ANOVA, Fig.3E). This demonstrated that the PKC inhibitor blocked ethanol effects on the decay constant.

We further confirmed the role of PKC at a lower concentration (50 mM) ethanol as a comparison to 100 mM. We found that 50 mM ethanol significantly shifted V_{50} to a more hyperpolarized membrane potential ($F_{1,10}=12.20$, $p=0.0058$, 2-way ANOVA; $p<0.01$, Bonferroni post hoc test, Fig. 3Gi) but there was no hyperpolarizing shift when MPI was

added in the internal solution (Fig. 3Gii). There was a significant interaction between ethanol and MPI treatment ($F_{1,10}$=8.701, p=0.0145, 2-way ANOVA), demonstrating that PKC inhibition blocks ethanol effects on the hyperpolarizing shift in the inactivation curve.

PMA Replicates Key Features of the Ethanol Effects on $Ca_V3.2$

The sensitivity of $Ca_V3.2$ current inactivation to PKC blockade led us to perform a further assessment of the role of PKC in mediating ethanol effects on these channels. To do this, we used a PKC activator, PMA, to activate PKC in recorded cells. After ten minute perfusion in the recording chamber, we found that 100 nM PMA produced a strong hyperpolarizing shift in the inactivation curve, but 1 μM PMA had no effect (Fig. 4A–D). We found PMA had a significant main effect on V_{50} ($F_{1,27}$=30.22, p<0.0001, 2-way ANOVA) and a significant interaction between PMA and concentration ($F_{1,27}$=16.98, p=0.0003, 2-way ANOVA). 100 nM PMA significantly shifted V_{50} to a more negative membrane potential (p<0.0001, Bonferroni post hoc test), but 1 μM PMA had no effect (Fig. 4E). This demonstrated that higher and lower concentrations of PMA had different effects on V_{50}. Similarly, we found that 100 nM PMA reduced T current, but 1 μM PMA increased the current. There was a significant main effect of concentration ($F_{1,27}$=10.69, p=0.0029, 2-way ANOVA) and a significant interaction between PMA and concentration ($F_{1,27}$=36.70, p<0.0001, 2-way ANOVA). 100 nM PMA reduced T current density (p<0.0001, Bonferroni post hoc test) but 1 μM PMA significantly increased current density (p<0.01, Bonferroni post hoc test, Fig. 4F). All experiments were performed at physiological temperature (30–34°C), and we also observed that 100 nM PMA had no effect on V_{50} and current density (n=6, p>0.05) near room temperature (22–27°C).

PMA Effects on Rise Time, Decay Constant and Estimated Charge

We characterized the rise time of the $Ca_V3.2$ current as the slope (nA/ms) of the line from baseline to the peak current. We found PMA had a significant main effect on rise slope ($F_{2,30}$=17.35, p<0.0001, 2-way ANOVA), rise time ($F_{2,30}$=12.68, p=0.0001, 2-way ANOVA) and decay constant ($F_{2,30}$=9.373, p=0.0007, 2-way ANOVA). 1 μM PMA significantly increased the rise slope (p<0.01, Bonferroni post hoc test, Fig.5A) and decreased the decay constant (p<0.05, Bonferroni post hoc test, Fig. 5C). Both 100 nM and 1 μM PMA significantly reduced the rise time, respectively (p<0.01 and p<0.05, Bonferroni post hoc test, Fig.5B).

We analyzed the estimated charge, or amount of current flowing through activated $Ca_V3.2$ channels, to determine if the relative charge in the different experimental conditions was consistent with our current density observations. We found PMA had a significant main effect on charge ($F_{1,26}$=36.74, p<0.0001, 2-way ANOVA) and a significant interaction between PMA and concentration ($F_{1,26}$=19.84, p=0.0001, 2-way ANOVA). 100 nM PMA significantly reduced charge (p<0.0001, Bonferroni post hoc test) but 1 μM PMA had no effect (p>0.05, Bonferroni post hoc test. Fig. 5D). The reduction in charge by 100 nM PMA was consistent with the reduction of current density induced by 100 nM PMA (Fig. 4F). However, 1 μM PMA modulated channel gating kinetics by producing significantly faster current decay constants, but it had no effect on the amount of charge through T channels (Fig. 5D). Thus, even though higher concentration of PMA increased the overall current

density, it had no effect on the amount of charge through $Ca_V3.2$ channels. Conversely, the lower concentration of PMA appeared to reduce both current density and charge.

In order to determine whether the PMA effect was through the PKC pathway, MPI was added in the internal solution. There was no hyperpolarizing shift in the inactivation curve in the presence of MPI (Fig. 5E). We found a significant main effect of PMA on V_{50} ($F_{1,22}$=16.27, p=0.0006, 2-way ANOVA) and a significant interaction between 100 nM PMA and MPI ($F_{1,22}$=18.45, p=0.0003, 2-way ANOVA). 100 nM PMA significantly shifted V_{50} to a more negative membrane potential (p<0.0001, Bonferroni post hoc test) but the effect was blocked when MPI was added in the internal solution. This result demonstrated that the effect of lower concentration of PMA on V_{50} is through the activation of PKC, producing identical effects to those observed in response to 100 mM ethanol. To assess the possibility of a common mechanistic path, we studied whether 100 nM PMA occluded the ethanol effect. We found that there was a significant difference between groups on the V_{50} ($F_{2,9}$=6.026, p=0.0218, 1-way ANOVA). A Bonferroni post hoc test showed significant differences between baseline and 100 nM PMA (p<0.05); baseline and 100 nM PMA plus 100 mM ethanol (p<0.05) but no significant difference between two treatment groups (p>0.05, Fig. 5F), illustrating that 100 nM PMA could occlude the effects of ethanol.

Ethanol Produces PKC-dependent Modulation of $Ca_V3.2$ in DRG Neurons

We next replicated our findings in a neuronal system. While thalamic neurons express native T-type currents, the relative distribution of T-type channels is better characterized in DRG neurons, where $Ca_V3.2$ is reported to be the predominant T channel isoform (Lee et al., 2009; Talley et al., 1999). Given the specificity of our observed effects on $Ca_V3.2$, we therefore conducted whole cell recordings of native currents in cultured DRG neurons to determine whether the ethanol effects that we observed in HEK cell lines showed the same form. In order to electrically isolate the T current from high voltage-gated calcium channels (HVA), currents were evoked at −50mV from holding potentials ranged from −135mV to −60 mV (the threshold of activation of HVA channels is around −40 mV and peaks at −10 to 0 mV). We further blocked any residual HVA current by the addition of 8 μM Nimodipine in the extracellular solution. We found that ethanol shifted the inactivation to a more hyperpolarized value (Fig. 6A). This effect was blocked by the PKC inhibitor (Fig. 6B). There were a significant main effect of ethanol on V_{50} V_{50} ($F_{1,30}$=4.990, p=0.0331, 2-way ANOVA) and a significant interaction between ethanol and MPI treatment ($F_{1,30}$=9.832, p=0.0038, 2-way ANOVA). Ethanol significantly shifted V_{50} to a more negative membrane potential (p<0.001, Bonferroni post hoc test, Fig. 6C) but 1 μM PMA had no effect as with the cell lines. It illustrated that MPI could block the ethanol effect on $V_{50.}$ We also found ethanol significantly reduced current density ($F_{1,30}$=7.430, p=0.0106, 2-way ANOVA, p<0.05, Bonferroni post hoc test, Fig.6D) but there was no interaction between ethanol and MPI treatment.

We then tested whether PMA had the same effects in DRG neurons as we observed in $Ca_V3.2$ channels from the HEK cell lines (Fig. 7). The representative traces illustrate that 100 nM PMA decreased the current, but 1 μM PMA increased the current. These effects partially recovered upon washout (Fig. 7A, C). 100 nM PMA significantly shifted the

inactivation curve in the hyperpolarized direction, but 1 μM PMA had no effect on inactivation (Fig. 7B, D). We found that 100 nM PMA significantly shifted V_{50} to a more negative membrane potential ($F_{1,25}$=5.038, p=0.0339, 2-way ANOVA; p<0.01, Bonferroni post hoc test, Fig.7E) but 1 μM PMA had no effect. Also there was a significant interaction between PMA and concentration ($F_{1,25}$=6.646, p=0.0162, Fig.7E). There was a significant main effect of concentration on current density ($F_{1,32}$=15.51, p=0.0004, 2-way ANOVA) and a significant interaction between PMA and concentration ($F_{1,32}$=16.21, p=0.0003, 2-way ANOVA). 100 nM PMA significantly decreased current density, but 1 μM PMA increased current density (p<0.05 for 100 nM PMA and p<0.01 for 1 μM PMA, Bonferroni post hoc test, Fig.7F). Taken together, this demonstrates that lower and higher concentrations of PMA had different effects on the V_{50} measure of voltage dependency as well as on current density.

The effects of PMA on decay constant and charge are concentration dependent as well. 1 μM PMA significantly reduced decay constant ($F_{1,28}$=4.396, p=0.0452, 2-way ANOVA; p<0.05, Bonferron post hoc test, Fig.7G) and charge ($F_{1,32}$=4.252, p=0.0474, 2-way ANOVA, p<0.01, Bonferron post hoc test, Fig.7H), illustrating that 100 nM PMA reduced the estimated charge through native T-channels in DRG neurons while 1 μM PMA showed no significant effect. Thus, the charge reduction due to the lower concentration of PMA appears to reflect the measured differences in current density. Moreover, the higher concentration of PMA produced significantly faster channel inactivation without affecting charge, even though current density was increased.

DISCUSSION

Ethanol inhibits T-current in both HEK ($Ca_V3.2$) and DRG Neurons

Our study was focused on the acute effects of ethanol on T-channels, and on determining the underlying cellular mechanism of the observed effects. We found that only one T channel isoform, $Ca_V3.2$, was affected by ethanol, first by studying HEK cells expressing $Ca_V3.2$, and separately in DRG neurons enriched in $Ca_V3.2$. We observed that ethanol produced a hyperpolarizing shift in the steady-state inactivation curve in both $Ca_V3.2$ channels and DRG neurons, but it did not affect the activation curve, suggesting that the window current would overall be reduced due to the hyperpolarizing shift in steady-state inactivation, which should yield a reduction in T-channel availability near resting membrane potential. Ethanol inhibition of $Ca_V3.2$ channels appears to be state dependent, possibly through stabilizing the channels in their inactivated state (Joksovic et al., 2010). In the current study, we were able to identify $Ca_V3.2$ as a specific target of ethanol, acting through PKC. Our study goes further to clarify differences in the literature on the nature and direction of PKC effects in neural systems.

Ethanol Effects on T-Current Fit a Pattern of Anesthetic Modulation

T-channels are located throughout the spinothalamic pathway, and contribute to the encoding of nociceptive signals from peripheral sensory neurons to the cortex (Carbone and Lux, 1984). Ethanol has known analgesic and anesthetic effects (McCracken et al., 2010; Ralevski et al., 2010). The effect of ethanol on T-current has similarities with the effect

produced by other general anesthetics on native T-current in peripheral and central neurons (Joksovic et al., 2005a,b; Todorovic et al., 2000). For example, the general anesthetic 1-octanol inhibits native T-current in neuronal systems, including DRG cells (Todorovic and Lingle, 1998), hippocampal neurons (Takahashi et al., 1989) and thalamic relay neurons (Llinás et al., 2007). Our results further suggest that $Ca_V3.2$ channels can be considered a novel target of the anesthetic effects of ethanol.

Ethanol Effects on T-type Current are Mediated by PKC

We found that a PKC inhibitor blocked the hyperpolarizing shift in the inactivation and the faster decay constant produced by ethanol in both $Ca_V3.2$ cells and DRG neurons. Also, ethanol significantly decreased current density, but we did not observe a blockade of the inhibitory effect of ethanol on current density by the PKC inhibitor in either $Ca_V3.2$ cells or DRG neurons. PKC seems to primarily mediate kinetic effects induced by ethanol, but the experiments did not support a role for PKC in mediating ethanol effects on current density. Taken together, our results suggested blockade of the PKC pathway in both the $Ca_V3.2$ cell line and in DRG neurons is sufficient to abolish the major effects of ethanol on T-currents, but the pharmacology used so far limits our ability to specify the specific isoform. Studies have shown that ethanol exposure for 1h increases PKCγ, PKCβ and PKCε peptide expression. In contrast, ethanol exposure for 4h only increases PKCγ and PKCβ but not PKCε protein levels (Kumar et al., 2010), and that 50 mM ethanol increases $GABA_A$ receptor α4 subunit expression via increases in PKCγ (Werner et al., 2011). Thus PKCγ is a candidate for our observed effects.

We observed that the lower concentration of PMA reduced current density, accompanied by a hyperpolarizing shift in the inactivation curve, similar to the effects of ethanol. However, the higher concentration of PMA increased current density and did not shift the inactivation curve. This suggested that the effects of ethanol can be mimicked by the lower concentration of PMA, through the activation of the PKC pathway. We further calculated the charge by integrating the total area under the curve and found that a lower concentration of PMA reduced charge, while higher concentration of PMA did not. This suggested that reduction of charge by the lower concentration of PMA was due mainly to the reduction of current amplitude. Although we found that higher concentration of PMA modulated channel gating kinetics (reflected by significantly faster current decay constants), there was no significant effect on charge in both HEK ($Ca_V3.2$) cells and native DRG neurons. Thus, while excitability changed due to effects on current density and altered inactivation, total charge did not appear to change with application of higher concentration of PMA.

Studies of PKC-dependent modulation of T current have yielded complex results across different preparations. For example, PKC activation in neonatal rat ventricular myocytes has been shown to potentiate T-current (Furukawa et al., 1992), while reducing T-current in rat DRG neurons (Schroeder et al., 1990), canine Purkinje cells (Tseng and Boyden, 1991), NIH-3T3 fibroblast cells(Pemberton et al., 2000), and GH3 cells (Marchetti and Brown, 1988). Studies in reconstituted Xenopus oocytes showed that 200 nM PMA potently enhanced the current amplitude of $Ca_V3.2$ T-channels, but 10 and 100 nM PMA inhibits T-current (Park et al., 2003), The precise mechanism underlying the differential modulation of

T-channel activity by PKC is not clear, but up or down regulation of PKC is dependent on the concentration of PMA. Our results indicate that 100 nM PMA activates PKC, since the PKC inhibitor blocked the PMA effect. The opposite effect of 1 μM PMA on V_{50} could be due to down regulation of PKC induced by a higher concentration of PMA. Activation of different isoforms of PKC, or difference in the modulation of available phosphorylation sites might be another reason for the concentration sensitive effects of PMA on T-channel activity. Phosphorylation of PKC may act in a concentration dependent way by progressively revealing multiple phosphorylation sites, either in the channel itself or in accessory proteins (Dang et al., 2001). This in turn may induce conformational changes that could modify the functional properties of the channel and lead to a higher probability of channel opening.

Studies of PKC have previously been performed at different temperatures, which may further obscure potential PKC effects across studies because PKC effects are highly temperature dependent (Schroeder et al., 1990). Interestingly, we did not observe effects on V_{50} or current density by 100 nM PMA (n=6) at room temperature (22–27 °C), while we did observe effects at physiological temperatures (32–34°C). This is consistent with the findings of Chemin et al (Chemin et al., 2007), who reported that kinase modulation of T-channels was temperature dependent. PKC translocation to the plasma membrane (where T –channels display their activity) induced by 100 nM PMA was observed at 37°C, but it was less apparent when the experiments were performed at room temperature (Chemin et al., 2007). Some studies (Schroeder et al., 1990) have indicated that at 32 °C, 10 nM and 100 nM PMA decreased T-current, and elevated temperatures (>29 °C) are required for inhibition by PMA. This temperature dependence could be due to differences in kinase translocation, which is impaired at room temperature (Chemin et al., 2007; Lehel et al., 1996).

Our study reveals that $Ca_V3.2$ is a novel target of ethanol. The main effects of ethanol on T current appear to occur through the $Ca_V3.2$ isoform and are due to activation of the PKC pathway, with a major effect being the hyperpolarized shift in inactivation. Our results showed that the major effects of ethanol could be abolished by the PKC peptide inhibitor, and could be mimicked by the PKC activator, PMA, when applied at lower concentrations. The role of PKC in response to acute ethanol treatment has been explored in cultured cells and *in vivo* (Ron et al., 2000). However, we found that the cellular effects of increasing PKC activity were shown to be more complex than originally envisioned, likely due to the complexity of the PKC pathway. The enhanced current due to higher concentration PMA may represent a unique molecular switch that will promote changes in excitability under conditions of higher PKC activity. Through PKC interactions that may elicit differing levels of PKC activation, ethanol is likely to exert a variety of interesting effects on PKC dependent processes.

Acknowledgments

We thank Dr. Edward Perez-Reyes for kindly providing the HEK 293 ($Ca_V3.1$, $Ca_V3.2$ and $Ca_V3.3$) cell lines. This work is supported by NIAAA AA014106, AA017056, AA016852, AA016852-04S1, and the Tab Williams Family fund.

REFERENCES

Bourinet E, Alloui A, Monteil A, Barrère C, Couette B, Poirot O, Pages A, McRory J, Snutch TP, Eschalier A, Nargeot J. Silencing of the Cav3.2 T-type calcium channel gene in sensory neurons demonstrates its major role in nociception. EMBO J. 2005; 24:315–324. [PubMed: 15616581]

Carbone E, Lux HD. A low voltage-activated, fully inactivating Ca channel in vertebrate sensory neurones. Nature. 1984; 310:501–502. [PubMed: 6087159]

Chemin J, Mezghrani A, Bidaud I, Dupasquier S, Marger F, C Barrère, Nargeot J, Lory P. Temperature-dependent Modulation of CaV3 T-type Calcium Channels by Protein Kinases C and A in Mammalian Cells. Journal of Biological Chemistry. 2007; 282:32710–32718. [PubMed: 17855364]

Chemin J, Monteil A, Bourinet E, Nargeot J, Lory P. Alternatively spliced alpha(1G) (Ca(V)3.1) intracellular loops promote specific T-type Ca(2+) channel gating properties. Biophys J. 2001; 80:1238–1250. [PubMed: 11222288]

Chen W-K, Liu IY, Chang Y-T, Chen Y-C, Chen C-C, Yen C-T, Shin H-S, Chen C-C. Ca(v)3.2 T-type Ca2+ channel-dependent activation of ERK in paraventricular thalamus modulates acid-induced chronic muscle pain. J Neurosci. 2010; 30:10360–10368. [PubMed: 20685979]

Coste B, Crest M, Delmas P. Pharmacological Dissection and Distribution of NaN/Nav1.9, T-type Ca2+ Currents, and Mechanically Activated Cation Currents in Different Populations of DRG Neurons. J Gen Physiol. 2007; 129:57–77. [PubMed: 17190903]

Coulter DA, Huguenard JR, Prince DA. Calcium currents in rat thalamocortical relay neurones: kinetic properties of the transient, low-threshold current. J Physiol (Lond). 1989; 414:587–604. [PubMed: 2607443]

Cribbs LL, Lee JH, Yang J, Satin J, Zhang Y, Daud A, Barclay J, Williamson MP, Fox M, Rees M, Perez-Reyes E. Cloning and characterization of alpha1H from human heart, a member of the T-type Ca2+ channel gene family. Circ Res. 1998; 83:103–109. [PubMed: 9670923]

Crunelli V, Lightowler S, Pollard CE. A T-type Ca2+ current underlies low-threshold Ca2+ potentials in cells of the cat and rat lateral geniculate nucleus. J Physiol (Lond). 1989; 413:543–561. [PubMed: 2557441]

Dang PM, Fontayne A, Hakim J, El Benna J, Périanin A. Protein kinase C zeta phosphorylates a subset of selective sites of the NADPH oxidase component p47phox and participates in formyl peptide-mediated neutrophil respiratory burst. J Immunol. 2001; 166:1206–1213. [PubMed: 11145703]

Furukawa T, Ito H, Nitta J, Tsujino M, Adachi S, Hiroe M, Marumo F, Sawanobori T, Hiraoka M. Endothelin-1 enhances calcium entry through T-type calcium channels in cultured neonatal rat ventricular myocytes. Circ Res. 1992; 71:1242–1253. [PubMed: 1327578]

Graef JD, Huitt TW, Nordskog BK, Hammarback JH, Godwin DW. Disrupted thalamic T-type Ca2+ channel expression and function during ethanol exposure and withdrawal. J Neurophysiol. 2011; 105:528–540. [PubMed: 21148095]

Graef JD, Nordskog BK, Wiggins WF, Godwin DW. An acquired channelopathy involving thalamic T-type Ca2+ channels after status epilepticus. J Neurosci. 2009; 29:4430–4441. [PubMed: 19357270]

Huguenard JR, McCormick DA. Simulation of the currents involved in rhythmic oscillations in thalamic relay neurons. J Neurophysiol. 1992; 68:1373–1383. [PubMed: 1279135]

Joksovic PM, Bayliss DA, Todorovic SM. Different kinetic properties of two T-type Ca2+ currents of rat reticular thalamic neurones and their modulation by enflurane. J Physiol (Lond). 2005a; 566:125–142. [PubMed: 15845580]

Joksovic PM, Brimelow BC, Murbartián J, Perez-Reyes E, Todorovic SM. Contrasting anesthetic sensitivities of T-type Ca2+ channels of reticular thalamic neurons and recombinant Ca(v)3.3 channels. Br J Pharmacol. 2005b; 144:59–70. [PubMed: 15644869]

Joksovic PM, Choe WJ, Nelson MT, Orestes P, Brimelow BC, Todorovic SM. Mechanisms of inhibition of T-type calcium current in the reticular thalamic neurons by 1-octanol: implication of the protein kinase C pathway. Mol Pharmacol. 2010; 77:87–94. [PubMed: 19846748]

Kumar S, Suryanarayanan A, Boyd KN, Comerford CE, Lai MA, Ren Q, Morrow AL. Ethanol Reduces GABAA α1 Subunit Receptor Surface Expression by a Protein Kinase Cγ-Dependent

Mechanism in Cultured Cerebral Cortical Neurons. Mol Pharmacol. 2010; 77:793–803. [PubMed: 20159950]

Lee JH, Daud AN, Cribbs LL, Lacerda AE, Pereverzev A, Klöckner U, Schneider T, Perez-Reyes E. Cloning and expression of a novel member of the low voltage-activated T-type calcium channel family. J Neurosci. 1999; 19:1912–1921. [PubMed: 10066244]

Lee WY, Orestes P, Latham J, Naik AK, Nelson MT, Vitko I, Perez-Reyes E, Jevtovic-Todorovic V, Todorovic SM. Molecular Mechanisms of Lipoic Acid Modulation of T-Type Calcium Channels in Pain Pathway. J Neurosci. 2009; 29:9500–9509. [PubMed: 19641113]

Lehel C, Oláh Z, Petrovics G, Jakab G, Anderson WB. Influence of various domains of protein kinase C epsilon on its PMA-induced translocation from the Golgi to the plasma membrane. Biochem Biophys Res Commun. 1996; 223:98–103. [PubMed: 8660386]

Llinás RR, Choi S, Urbano FJ, Shin H-S. Gamma-band deficiency and abnormal thalamocortical activity in P/Q-type channel mutant mice. Proc Natl Acad Sci USA. 2007; 104:17819–17824. [PubMed: 17968008]

Marchetti C, Brown AM. Protein kinase activator 1-oleoyl-2-acetyl-sn-glycerol inhibits two types of calcium currents in GH3 cells. Am J Physiol. 1988; 254:C206–210. [PubMed: 2447796]

McCracken ML, Borghese CM, Trudell JR, Harris RA. A transmembrane amino acid in the GABAA receptor β2 subunit critical for the actions of alcohols and anesthetics. J Pharmacol Exp Ther. 2010; 335:600–606. [PubMed: 20826568]

Monteil A, Chemin J, Leuranguer V, Altier C, Mennessier G, Bourinet E, Lory P, Nargeot J. Specific properties of T-type calcium channels generated by the human alpha 1I subunit. J Biol Chem. 2000; 275:16530–16535. [PubMed: 10749850]

Mu J, Carden WB, Kurukulasuriya NC, Alexander GM, Godwin DW. Ethanol Influences on Native T-Type Calcium Current in Thalamic Sleep Circuitry. J Pharmacol Exp Ther. 2003; 307:197–204. [PubMed: 12893844]

Nelson MT, Todorovic SM, Perez-Reyes E. The role of T-type calcium channels in epilepsy and pain. Curr Pharm Des. 2006; 12:2189–2197. [PubMed: 16787249]

Ohishi M, Takagi T, Ito N, Terai M, Tatara Y, Hayashi N, Shiota A, Katsuya T, Rakugi H, Ogihara T. Renal-protective effect of T-and L-type calcium channel blockers in hypertensive patients: an Amlodipine-to-Benidipine Changeover (ABC) study. Hypertens Res. 2007; 30:797–806. [PubMed: 18037772]

Park J-Y, Jeong S-W, Perez-Reyes E, Lee J-H. Modulation of Ca(v)3.2 T-type Ca2+ channels by protein kinase C. FEBS Lett. 2003; 547:37–42. [PubMed: 12860383]

Pemberton KE, Hill-Eubanks LJ, Jones SV. Modulation of low-threshold T-type calcium channels by the five muscarinic receptor subtypes in NIH 3T3 cells. Pflugers Arch. 2000; 440:452–461. [PubMed: 10954332]

Perez-Reyes E. Molecular physiology of low-voltage-activated t-type calcium channels. Physiol Rev. 2003; 83:117–161. [PubMed: 12506128]

Perez-Reyes E, Cribbs LL, Daud A, Lacerda AE, Barclay J, Williamson MP, Fox M, Rees M, Lee JH. Molecular characterization of a neuronal low-voltage-activated T-type calcium channel. Nature. 1998; 391:896–900. [PubMed: 9495342]

Ralevski E, Perrino A, Acampora G, Koretski J, Limoncelli D, Petrakis I. Analgesic effects of ethanol are influenced by family history of alcoholism and neuroticism. Alcohol Clin Exp Res. 2010; 34:1433–1441. [PubMed: 20497133]

Ron D, Vagts AJ, Dohrman DP, Yaka R, Jiang Z, Yao L, Crabbe J, Grisel JE, Diamond I. Uncoupling of betaIIPKC from its targeting protein RACK1 in response to ethanol in cultured cells and mouse brain. FASEB J. 2000; 14:2303–2314. [PubMed: 11053252]

Schroeder JE, Fischbach PS, McCleskey EW. T-type calcium channels: heterogeneous expression in rat sensory neurons and selective modulation by phorbol esters. J Neurosci. 1990; 10:947–951. [PubMed: 2156966]

Takahashi K, Wakamori M, Akaike N. Hippocampal CA1 pyramidal cells of rats have four voltage-dependent calcium conductances. Neurosci Lett. 1989; 104:229–234. [PubMed: 2554221]

Talley EM, Cribbs LL, Lee JH, Daud A, Perez-Reyes E, Bayliss DA. Differential distribution of three members of a gene family encoding low voltage-activated (T-type) calcium channels. J Neurosci. 1999; 19:1895–1911. [PubMed: 10066243]

Todorovic SM, Lingle CJ. Pharmacological properties of T-type Ca2+ current in adult rat sensory neurons: effects of anticonvulsant and anesthetic agents. J Neurophysiol. 1998; 79:240–252. [PubMed: 9425195]

Todorovic SM, Perez-Reyes E, Lingle CJ. Anticonvulsants but not general anesthetics have differential blocking effects on different T-type current variants. Mol Pharmacol. 2000; 58:98–108. [PubMed: 10860931]

Tseng GN, Boyden PA. Different effects of intracellular Ca and protein kinase C on cardiac T and L Ca currents. Am J Physiol. 1991; 261:H364–379. [PubMed: 1652211]

Werner DF, Kumar S, Criswell HE, Suryanarayanan A, Fetzer JA, Comerford CE, Morrow AL. PKCγ is required for ethanol-induced increases in GABAA receptor α4 subunit expression in cultured cerebral cortical neurons. Journal of Neurochemistry. 2011; 116:554–563. [PubMed: 21155805]

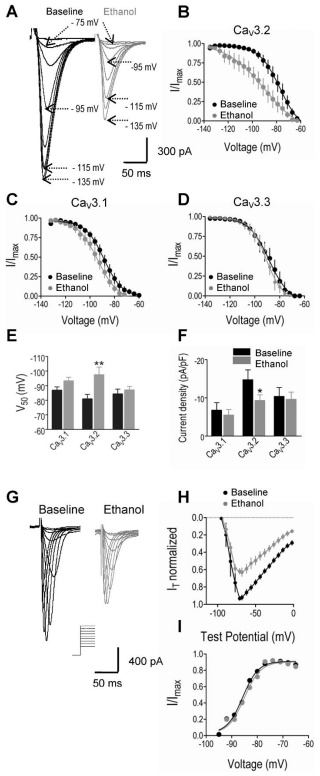

Fig. 1.

Ethanol selectively inhibits $Ca_V3.2$ channels recorded from human embryonic kidney (HEK) 293 cell lines. (A) Representative current inactivation traces of $Ca_V3.2$ channels recorded before and at ten minutes after the bath application of 100 mM ethanol. Current inactivation was elicited at −50 mV from holding potentials starting from −135 to −60 mV for one second. (B) 100 mM ethanol induced a strong hyperpolarizing shift in the steady-state inactivation curve in the whole cell current (fitted with Boltzmann equation). (C, D) 100 mM ethanol had no significant effect on steady-state inactivation curves in currents recorded from HEK cells expressing $Ca_V3.1$ and $Ca_V3.3$ channels. (E) V_{50} derived from the inactivation curve was significantly shifted to a more hyperpolarized membrane potential after application of 100 mM ethanol in the cells expressing $Ca_V3.2$ channels. (n =11, $p<0.01$, **, paired *t*-test) but it did not change in $Ca_V3.1$ or $Ca_V3.3$ currents. (F) 100 mM ethanol decreased current density in $Ca_V3.2$ channels but had no effect in $Ca_V3.1$ and $Ca_V3.3$ channels (n=10, $p<0.05$, *, paired *t*-test). (G) Representative current activation traces were elicited from −95 mV to 0 mV in 6 mV increments from a holding potential of −135 mV for one second. (H) Average I-V relationship before and during the application of 100 mM ethanol. The I-V curve was plotted with normalized peak current against the command potentials. After 10 minutes application of ethanol in the bath, peak current reduced about 32% (n=7, $p<0.001$, paired *t*-test). (I) Steady-state activation was deduced from I-V curves presented in (H) and fitted with Boltzmann equation. V_{50} Derived from activation curve showed no significant changes after application of 100 mM Ethanol. *$p<0.05$; **$p<0.01$.

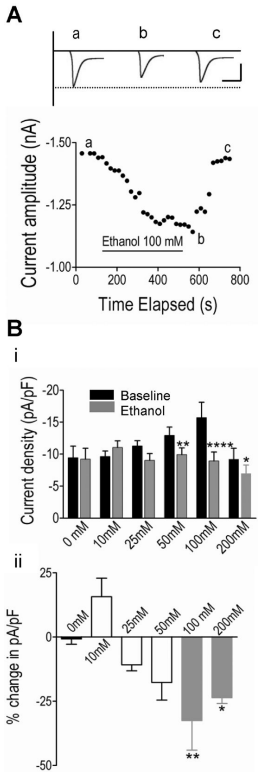

Fig. 2.

Biphasic, dose-dependent effect of ethanol on current density in $Ca_V3.2$ channels from HEK cell lines. (A) Representative traces and time course showing the effects of 100 mM ethanol on $Ca_V3.2$ channels (scale bar: 50 msec, 1 nA). Peak reduction was reached 10 minutes after applying ethanol. (Bi) 50, 100 and 200 mM ethanol significantly reduced current density (2-way ANOVA followed by Bonferroni post hoc test). (Bii) The percentage changes of normalized current density obtained between the ethanol and control current measured in the same cell showed only 100 and 200 mM ethanol were significantly different from control (1-way ANOVA followed by Dunnett's post hoc test). *p<0.05; **p<0.01;**** p<0.0001.

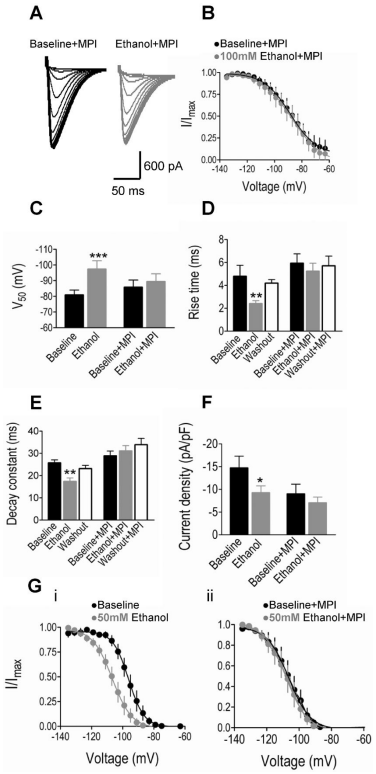

Fig. 3.

PKC mediated ethanol effects on kinetics and current density of $Ca_V3.2$ currents recorded from HEK cell lines. Myristoylated Protein Kinase C (PKC) peptide inhibitor (MPI: 50 μM) was delivered through the pipette internal solution. (A) Representative inactivation $Ca_V3.2$ current traces recorded in the absence, presence of 100 mM ethanol in the recording chamber with the PKC inhibitor in the internal solution (the same protocol as was used in Fig.1). (B) 100 mM ethanol showed no hyperpolarizing shift in the steady-state inactivation curve in $Ca_V3.2$ channels with PKC inhibitor in the internal solution. (C) Ethanol significantly shifted V_{50} to a more hyperpolarized membrane potential. MPI blocked ethanol effects. ((D,E,F) Ethanol produced significantly faster rise time, decay constant and reduction in current density, MPI blocked ethanol effects on decay constant. ((Gi) 50 mM ethanol produced a hyperpolarizing shift in the steady-state inactivation curve in $Ca_V3.2$ channels (fitted with Boltzmann equation). V_{50} derived from the inactivation curve was significantly shifted to a more hyperpolarized membrane potential. (Gii) 50 mM ethanol showed no hyperpolarizing shift in the steady-state inactivation curve in $Ca_V3.2$ channels when 50 μM MPI was added in the internal solution. *p<0.05; **p<0.01;*** p<0.001.

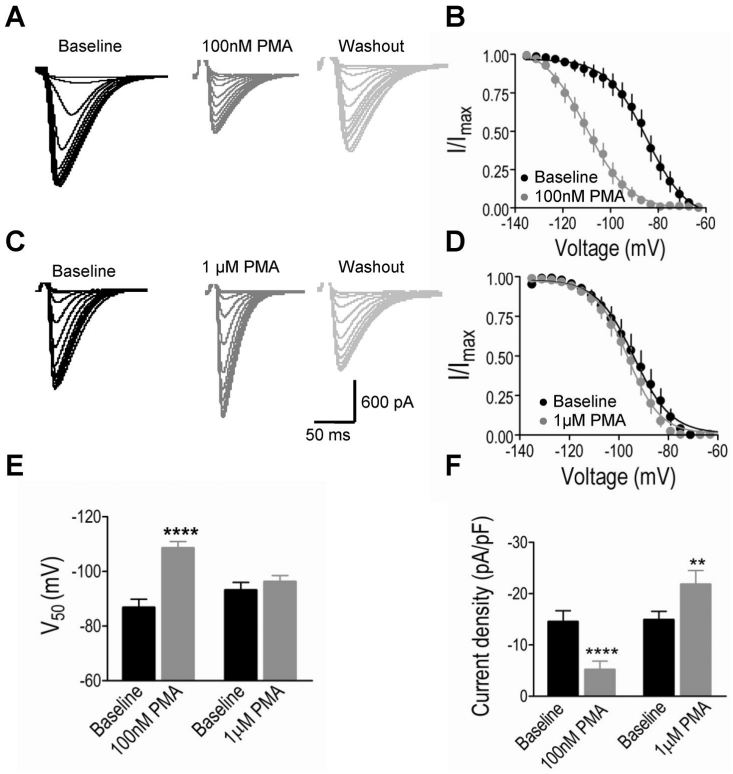

Fig. 4.

Lower (100 nM) and higher (1 μM) concentrations of phorbol 12-myristate 13-acetate (PMA) produce different effects on steady-state inactivation and current density of $Ca_V3.2$ channels from HEK cell lines. (A, C) Representative inactivation $Ca_V3.2$ current traces recorded in the absence, and ten minutes after application in the recording chamber of 100 nM, 1 μM PMA and wash out with ACSF (the same inactivation protocol as was used in Fig. 1). (B) 100 nM PMA induced a strong hyperpolarizing shift in steady-state inactivation curve in $Ca_V3.2$ channels. (D) 1 μM PMA had no effect on the inactivation curve. (E) 100 nM PMA significantly shifted V_{50} to a more hyperpolarized membrane potential, but 1 μM PMA had no significant effect. (F) 100 nM PMA significantly reduced current density but 1 μM PMA increased current density. **p<0.01;**** p<0.0001.

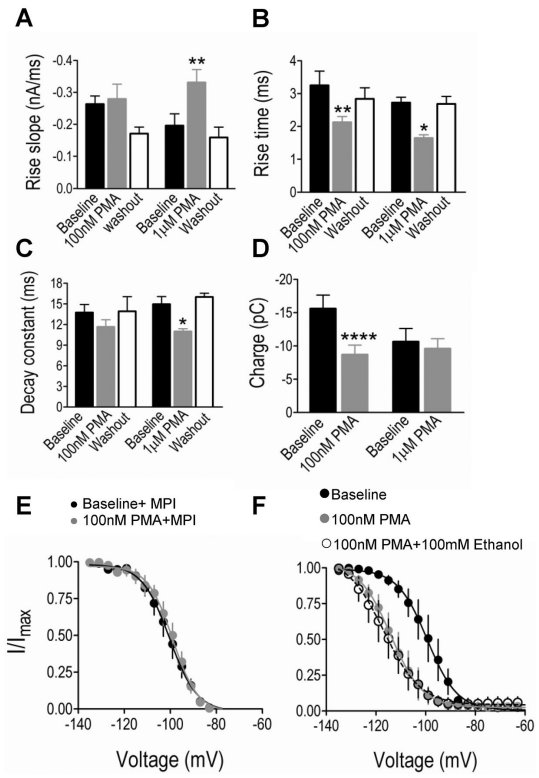

Fig. 5.

The effects of lower (100 nM) and higher (1 μM) concentrations of PMA on kinetic properties in $Ca_V3.2$ currents recorded from HEK cell lines. (A) 1 μM PMA significantly increased rise slope. (B) Both 100 nM PMA 1 μM PMA significantly reduced rise time. (C) 1 μM PMA produced a significantly faster decay constant that recovered upon washout. (D) 100 nM PMA significantly reduced charge. ((E) 50 μM MPI blocked hyperpolarizing shift in steady-state inactivation curve induced by 100 nM PMA. (F). 100 nM PMA induced a hyperpolarizing shift in steady-state inactivation curve, but no further shift was observed after adding 100 mM ethanol, demonstrating occlusion of 100 nM PMA on ethanol effects. *p<0.05;**p<0.01;**** p<0.0001.

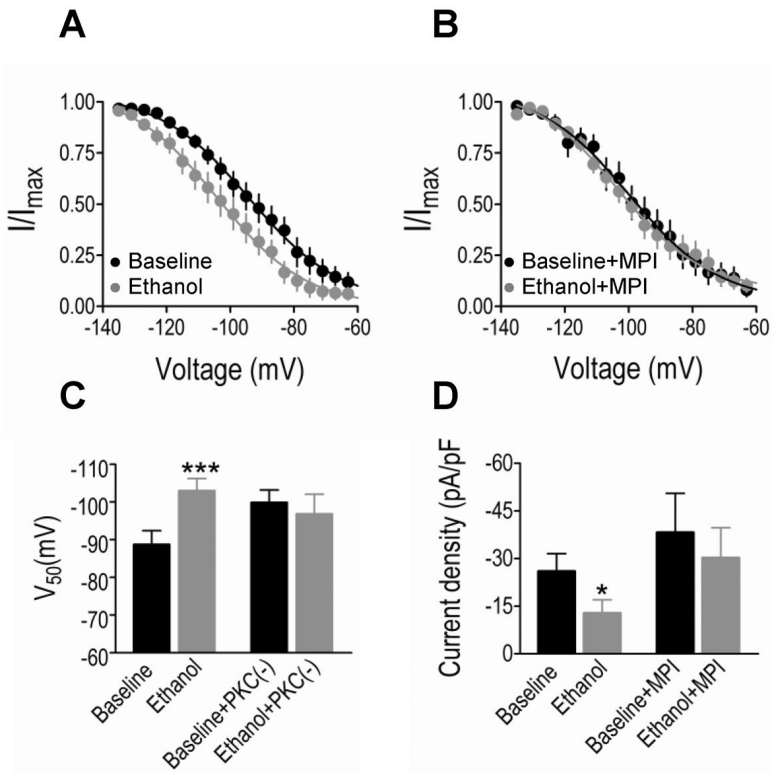

Fig. 6.

PKC mediated inhibition of ethanol on T current in dorsal root ganglion (DRG) neurons. (A) 100 mM ethanol produced a hyperpolarizing shift in the inactivation curve (the same protocol as was used in Fig 1). (B) There was no hyperpolarizing shift after application of 100 mM ethanol while the PKC peptide inhibitor (MPI: 50 μM) was in the internal solution. (C) Ethanol significantly shifted V_{50} to a more hyperpolarized membrane potential, and it was blocked by MPI. (D) Ethanol significantly reduced current density.
*p<0.05;***p<0.001.

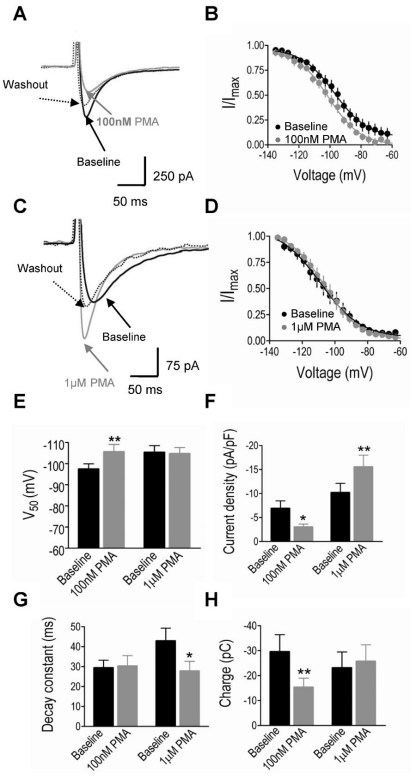

Fig. 7.

The effects of lower (100 nM) and higher (1μM) concentrations of PMA on T-type currentsin DRG neurons. (A) Representative T current traces recorded in the absence and ten minutes after application of 100 nM PMA in the recording chamber, and after washout with ACSF. 100 nM PMA reduced T current, which partially recovered upon washout with ACSF. (B) 100 nM PMA shifted the steady-state inactivation curve to a more hyperpolarized membrane potential. (C) 1 μM PMA increased T current amplitude, which recovered upon washout with ACSF. (D) 1 μM PMA had no effect on the steady-state inactivation curve. (E) 100 nM PMA significantly shifted V_{50} to a more hyperpolarized membrane potential, but 1 μM PMA had no effect. (F) 100 nM PMA significantly reduced but 1 μM PMA significantly enhanced current density. (G) 1μM PMA significantly produced a faster decay constant. (H) 100 nM PMA significantly reduced charge.